Journal of Power Sources 247 (2014) 256–263

Contents lists available at ScienceDirect

Journal of Power Sources

journal homepage: www.elsevier.com/locate/jpowsour

Passive hydrogen recovery schemes using a vacuum ejector in a proton exchange membrane fuel cell system

Jenn-Jiang Hwang*

Department of Greenergy, National University of Tainan, Tainan, Taiwan

HIGHLIGHTS

- A vacuum ejector fluidly connected to the anode outlet entrains the unused hydrogen into the supply line.
- The passive hydrogen delivery scheme contains a continuous-flow mode and a pulse-flow mode.
- The anode stoichiometry has been stabilized in the range of 1.4–1.6 with an entrainment ratio of 40–50%.
- The reliability of the passive scheme has been verified by an approximate 1-h test.

ARTICLE INFO

Article history:
Received 24 June 2013
Received in revised form
28 August 2013
Accepted 28 August 2013
Available online 6 September 2013

Keywords:
Vacuum ejector
Hydrogen recirculating scheme
Entrainment ratio
Proton exchange membrane fuel cell

ABSTRACT

The present work describes the development of a passive hydrogen-recirculating scheme for the anode of a proton exchange membrane (PEM) fuel cell system. A vacuum ejector is fluidly connected to the stack anode outlet to entrain the unused hydrogen into the main hydrogen supply. A combination of a continuous-flow mode and a pulse-flow mode is employed to cover a wide range of power consumption. The former deals with the normal and high stack power conditions, while the latter is active only at low stack power. Transient results showed that the hydrogen anode stoichiometry has been successfully stabilized in the range of 1.4–1.6 with an entrainment ratio of 40–50% under the constant system load of 1.45 kW. In addition, the reliable operation of the PEM fuel cell system without any failure during the approximate 1-h test indicates the stability and reliability of the present hydrogen recovery scheme.

1. Introduction

Proton exchange membrane (PEM) fuel cells have been widely used as the primary power source in transportation applications such as scooters, sedans, buses, boats, and space crafts, owing to their numerous advantages over the conventional power sources such as short startup time, compact system volume, low emission of pollutants, and relatively high system efficiency [1,2].

In a PEM fuel cell system, hydrogen is usually used as the fuel. Typically, the hydrogen circuit of a PEM fuel cell is operated in a dead-end mode, in which the anode outlet is closed and the hydrogen is consumed inside the anode compartment [3–5]. The dead-end mode of operation needs a high-purity hydrogen fuel gas, e.g., >99.99% hydrogen, and requires periodic purges to remove water generated in the reaction and other impurities in the hydrogen fuel gas. In addition, an alternative hydrogen delivery scheme of the flow-through mode has been widely used in the anode compartment of a PEM fuel cell. In this scheme, the hydrogen fuel gas flows through the anode continuously and only a portion of the hydrogen in the fuel gas is consumed with substantial amount of hydrogen contained in the exhaust gas from the anode. Therefore, the hydrogen utilization in the flow-through mode is lower than that in the dead-end mode. The general treatment of the unused hydrogen in the stack anode is to recirculate back to the anode counterpart by an electric pump [5–7]. However, the electric pump utilizes the electrical power generated by the fuel cell stack, thereby decreasing the overall efficiency. Therefore, it has been an ongoing challenge to provide an efficient method of reintroducing the unused hydrogen back into the main hydrogen passage. To address this challenge, vacuum ejectors have been used in fuel cell systems to introduce fuel from the fuel source to the fuel cell stack [2,8]. A vacuum ejector is a passive jet pump, which does not consume any electricity [9,10]. Instead, it uses the potential energy of the pressurized primary fluid to pump the secondary fluid by accelerating the primary fluid through the nozzle of the ejector, thus decreasing its pressure. In other words, the high-pressure

* Tel./fax: +886 62602205.
E-mail addresses: azaijj@mail.nutn.edu.tw, azaijj@gmail.com.

0378-7753/$ – see front matter © 2013 Elsevier B.V. All rights reserved.
http://dx.doi.org/10.1016/j.jpowsour.2013.08.126

motive fluid passes through the nozzle, where its pressure is dissipated in accelerating the fluid to a high velocity as it exits the mouth of the nozzle. The high velocity fluid stream exiting the nozzle entrains the relatively low-pressure fluid introduced at the suction inlet to the ejector. Entrainment of the low-pressure suction fluid with the motive fluid causes the suction fluid to move with the motive fluid. The two streams mix as they pass into the diffuser portion of the ejector. An additional advantage of an ejector is its rigid and simple construction, which makes it very reliable and long-lasting. Furthermore, an ejector has no moving parts and, thus, does not need any lubrication and requires very little maintenance [9]. However, the function of an ejector depends strongly on its geometry, which means that the ejector works only at a relatively narrow range of flow rates [2]. In addition, hydrogen must continuously be consumed in the fuel cell stack in order to work as a recirculation pump for a vacuum ejector.

The objective of the present work is to develop a passive hydrogen delivery scheme to effectively recover the unused hydrogen in the anode counterpart of a PEM fuel cell system. A vacuum ejector is fluidly connected to the stack anode outlet to entrain the unused hydrogen into the main hydrogen supply. Two different hydrogen supply schemes are employed to cover a wide range power consumption during the operation, which combines a continuous-flow mode and a pulse-flow mode in the hydrogen supply. The continuous-flow mode deals with the normal and the high stack power conditions, while the pulse-flow mode is active only when the stack power is outside the working range of the vacuum ejector [2].

2. System descriptions

2.1. Fuel cell generator

Fig. 1 shows a schematic of a PEM fuel cell generator, which consists of a PEM fuel cell stack, an airflow circuit, a coolant flow circuit, a power-conditioning module, and a hydrogen flow circuit. Except for the hydrogen flow circuit, all the other subsystems of the fuel cell generator have been illustrated in detail elsewhere [11–13]; thus, only some of the relevant features are briefly explained here.

The fuel cell stack is made up of 50 cells that contain two composite plates and a proton exchange membrane. The technical specifications of the fuel cell stack are given in Table 1. The airflow circuit provides filtered, conditioned air to the cathode of the fuel cell stack. It includes an air filter, an air blower, and a membrane

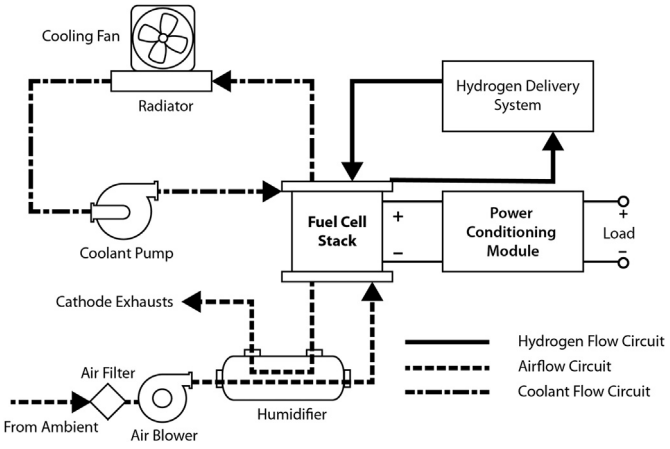

Fig. 1. Schematic drawing of the fuel cell generator.

Table 1
Technical specifications of the fuel cell stack.

Specifications	Value
Number of cells	50
Active area	150 cm^2
Rated net output	2000 W @ 36VDC
Cut-off voltage	28 VDC
Operating temperature	40–80 °C
Anode feeding	Gaseous hydrogen, 99.99% in purity
Cathode feeding	Ambient air
Coolant	Propylene glycol/DI water mixture (50%/50%)

humidifier. The air filter removes volatile gases and solid contaminates from the process airstream by chemical absorption using activated carbon media and mechanical filtration. The air blower acquired from Ametek has a variable speed motor controlled by a separate motor controller. The motor speed of the blower is a function of the DC power output of the fuel cell system [14,15]. The membrane humidifier produced by Perma transfers the heat and the humidity from the stack cathode exhaust to the inlet airstream [16,17]. The coolant flow circuit consists of a coolant pump and a radiator/fan assembly [18], which coordinates the fan speed and the pump speed to ensure an operating temperature of approximately 80 °C [19] in the fuel cell stack. The coolant is a mixture of 50% propylene glycol and 50% DI water, which provides a good thermal conductivity and cold-start properties. The power-conditioning module provides a proper interface between the stack power and the external load, which consists of a bidirectional DC/DC converter, a secondary (lithium-ion) battery, a programmable electronic load, and a power controller [20,21]. During a high power demand on the external load, the converter boosts the stack power to the DC bus, and the lithium-ion battery discharges to add the extra power to the DC bus. In contrast, when the external load power demand is less than the power generated by the fuel cell stack, the converter uses the extra stack power to charge the lithium-ion battery.

2.2. Hydrogen delivery circuit

Fig. 2 depicts the hydrogen flow circuit of the fuel cell generator. In contrast to the active electrical pump in our previous work [22], a passive jet pump, i.e., a vacuum ejector, is employed to recirculate the unused hydrogen in the anode counterpart. Note that the maximum power consumption of the electrical pump occupies about 10% of the auxiliary power of BOPs in a fuel cell system [22].

Fig. 3 shows a sectional view of the vacuum ejector, which comprises of a motive inlet, an entrainment inlet, and a discharge outlet. They are fluidly connected to the high-pressure fresh hydrogen supply (motive or primary flow), the unused hydrogen stream from the anode outlet (entrainment or secondary flow), and the hydrogen stream inlet (combined flow) of the stack anode, respectively. The throat diameter of the ejector is 1.0 mm. During the operation, fresh hydrogen enters the ejector from the motive inlet, and then drives and mixes with the recirculating flow by suction. The merger of the recirculated hydrogen stream *m2* and the pressurized fresh hydrogen stream *m1* thus forms the discharge hydrogen stream of the vacuum ejector *m3*. The discharge flow passes into the diffuser portion of the ejector, where the relatively high velocity of the mixed fluids is converted into static pressure. Thereafter, the hydrogen flow through the flow field channels of the anode results in a pressure drop between the anode inlet and the anode outlet, i.e., $P_{ai} - P_{ao}$. This pressure drop provides the driving force for moving the fuel through the anode flow field channels, which is closely related to the effectiveness of removing

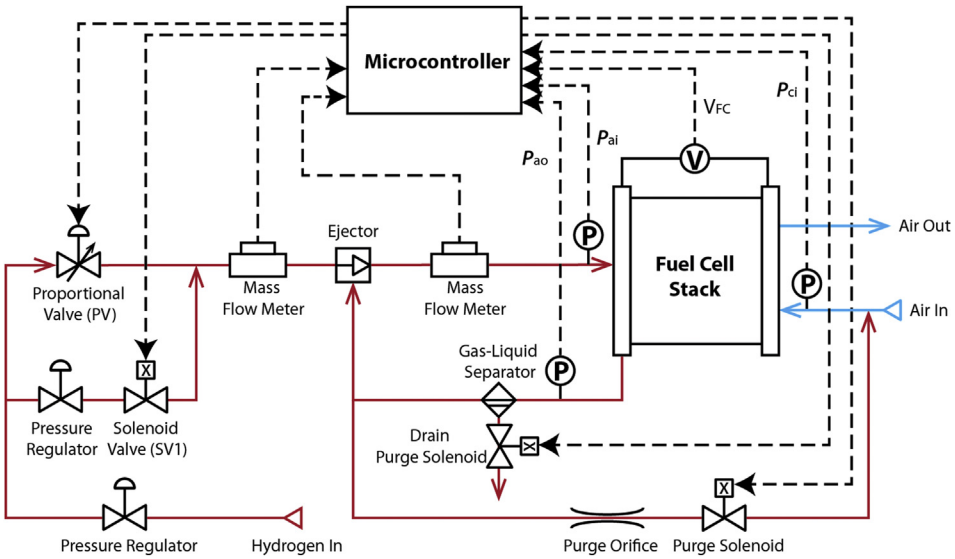

Fig. 2. Illustration of the hydrogen delivery circuit of the fuel cell generator.

the water droplets from these channels. During the operation, the variation in the feed pressure of the motive fluid by adjusting the proportional valve PV controls the ejector effectiveness.

As shown in Fig. 2, to avoid the accumulation of liquid water in the anode, the anode exhaust fuel gas passes through a gas/liquid separator installed in the recirculation circuit that removes the water contained in the unused hydrogen stream before reintroducing it into the main hydrogen passage [23]. Thereafter, a portion of the hydrogen/inert gas mixture is exhausted into the cathode inlet through an orifice along with a solenoid valve, which could help in increasing the humidity of the cathode inlet stream. This solenoid valve remains open whenever the fuel cell system is shut down, and allows the hydrogen in the circuit to vent when not in use. Such a mechanism prevents a vacuum from building up within the fuel delivery circuit, since any residual hydrogen would slowly react within the fuel cell stacks while the system is off. Table 2 lists the major components employed in the passive hydrogen delivery circuit.

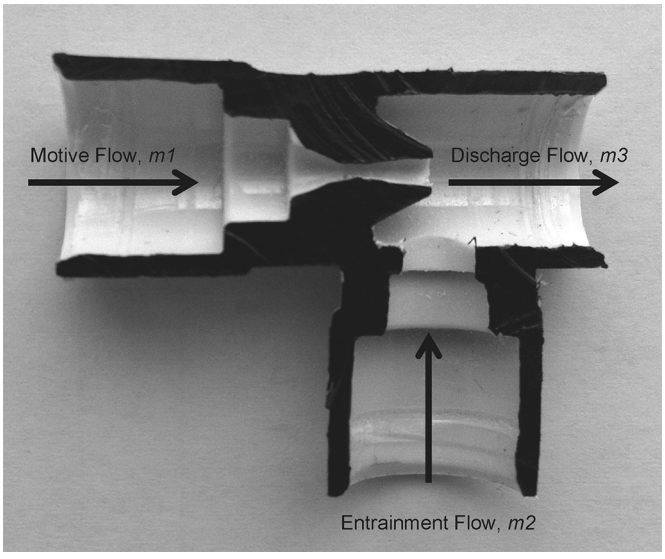

Fig. 3. Cut-view of the vacuum ejector.

3. Results and discussion

3.1. Ejector characteristics

Fig. 4 shows the flow characteristics of the ejector, illustrating the effect of the supply pressure, and hence the motive flow rate at the ejector inlet, on the entrainment flow rates and the vacuum pressure on the suction port. The supply pressure at the ejector varies from 0.02 to 0.4 MPa. Both the discharge port and the suction port of the ejector are open to the ambient. The experiments are carried out under unreactive conditions with compressed air as the working fluid.

As shown in Fig. 4, the motive flow rate *m1* increases with increasing supply pressure, such that the higher static pressures are converted to the higher flow rates. Moreover, the entrainment flow rate *m2* at the suction port increases with increasing supply pressure. Physically, the vacuum pressure at the suction port increases (in negative values) when the motive flow rate increases, which in-turn enhances the flow entrainment at the suction port and thus increases the entrainment flow rate. Consequently, the total flow rate through the discharge port increases with increasing supply pressure. Note that no entrainment flow is sensed on the suction port when the supply pressure is lower than 0.01 MPa (data not shown in Fig. 4). In other words, the supply pressure, and consequently the motive flow rate, should be higher than a threshold valve to effectively entrain the flow from the suction port [2]. During the design of the hydrogen delivery scheme utilizing the vacuum ejector, the airflow rate in Fig. 4 is

Table 2
Major components of the passive hydrogen delivery circuit.

Components	Quantity
Vacuum ejector	1
Proportional valve	1
Pressure regulator	2
Solenoid valve	3
Gas/liquid separator	1
Pressure sensor	3
Purge orifice	1
Mass flow meter	2
Microcontroller	1

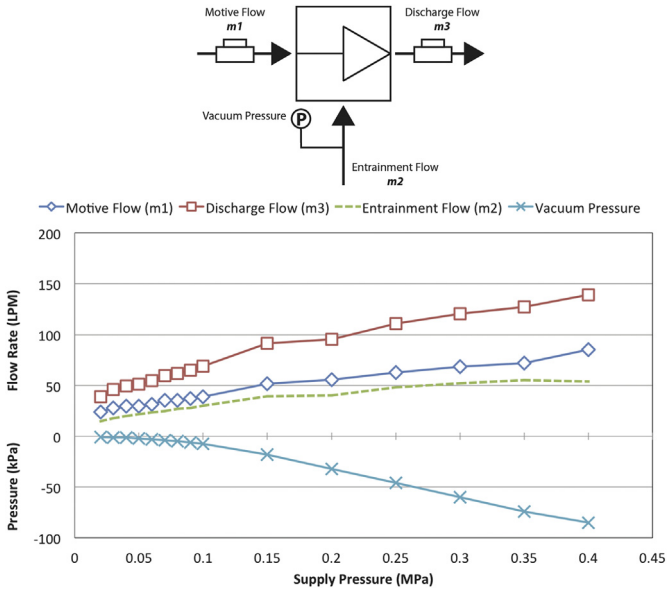

Fig. 4. Flow characteristics of the vacuum ejector.

converted to the hydrogen flow rate by using the Reynolds analogy [24].

3.2. Effect of stack power

For an ejector, hydrogen must continuously be consumed in the fuel cell stack in order to work as a recirculation pump. However, under the low stack power conditions, the hydrogen flow rate across the ejector is small. Therefore, according to the discussions above, the ejector cannot create a vacuum environment on the suction port to entrain the flow from the recirculation circuit. In addition, the small hydrogen flow cannot ensure an adequate removal of water droplets from the anode flow field channels. Thus, the continuous flow across the vacuum ejector would not be suitable for the low stack power conditions. The present work uses two different hydrogen delivery schemes for wide-ranging operation conditions. As shown in Fig. 5, the first scheme is a continuous-flow mode for the normal and high stack power conditions, while the second scheme uses the pulse flow to deal with the low stack power conditions.

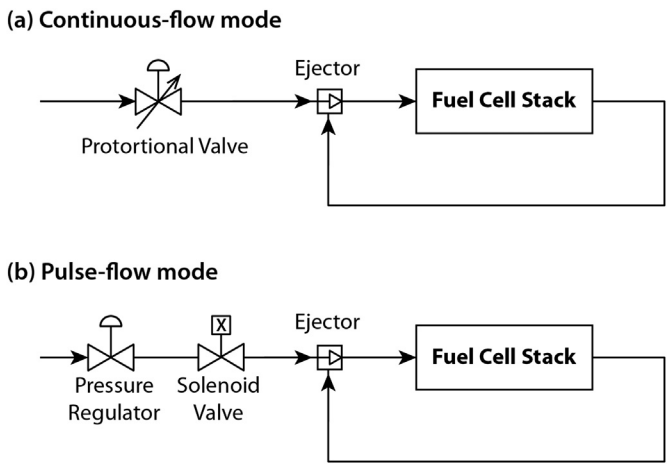

Fig. 5. Schematics of (a) continuous jet flow for high stack power (>600 W) and (b) pulsejet flow for low stack power (<600 W).

The continuous-flow mode comprises the following steps:

1. Determine the threshold stack power and thus the minimum hydrogen flow rate at which there is a sufficient driving force to remove the water droplets accumulated in the anode flow field channels.
2. A closing of the solenoid valve SV1 to direct hydrogen to the stack anode via the proportional valve PV to the fuel cell stack when the stack power is higher than the threshold value.
3. Commanding the proportional valve to increase/decrease the pressure of the hydrogen stream at the anode inlet when the stack power, and consequently the hydrogen flow rate through the vacuum ejector, increases/decreases.

Fig. 6 represents the typical results of the continuous-flow mode, which shows the hydrogen flow rate as a function of the stack power for $P_{stack} > 600$ W. During the operation of the fuel cell stack, the microcontroller controls the proportional valve to vary the amount of hydrogen supplied to the stack, such that the hydrogen anode stoichiometry is maintained at a preset level. Thus, the interaction of the pressure signals and the proportional valve causes the ejector to be loaded, and therefore capable of maintaining both a relatively uniform inlet hydrogen stream pressure to the stack anode and a relatively uniform hydrogen recirculation ratio. As shown in Fig. 6, all the three hydrogen flow rates increase with an increase in the stack power. In addition, the entrainment ratio keeps stable at 40%, and the hydrogen anode stoichiometry varies in a narrow range of 1.6–1.7. This implies that the pressurized hydrogen in the fuel supply line is sufficient to ensure the adequate entrainment of the recirculated fuel stream by the fresh fuel stream. In addition, the anode pressure difference created in the stack is sufficient for adequately removing the water droplets from the anode flow field channels and ensuring a stable stack operation.

In contrast to the continuous-flow mode, the pulse-flow mode is employed when the stack power is lower than the threshold value, as shown in Fig. 5(b). In this case, the microcontroller closes the proportional valve PV in the fuel supply line to direct hydrogen to the stack anode via the solenoid valve SV1. The methodology of the pulse-flow mode comprises of the following steps:

1. Initially opening the solenoid valve SV1 and supplying fuel to the fuel cell stack.
2. Completely closing the solenoid valve SV1 and keeping it closed to stop the hydrogen supply to the stack when the pressure difference between the anode inlet and the anode outlet is above a preset value A.
3. Opening the solenoid valve SV1 to restart the fuel supply to the stack when the pressure difference drops below another preset value B. The second preset threshold value B is lower than the first preset threshold value A.
4. The periodic opening and closing of the solenoid valve SV1 creates a pulsed hydrogen supply to the stack.

Fig. 7 shows a representative illustration of the transient pressure distribution at the anode outlet of the pulse-flow mode for the stack power of $P_{stack} = 300$ W. The actions of the solenoid valve SV1 are also shown. It can be seen that the anode outlet pressure increases sharply when the solenoid valve SV1 opens. This valve then closes quickly to stop the fuel supply to the stack. Thereafter, the anode outlet pressure gradually declines due to the fuel consumption by the hydrogen reduction reaction (HOR). As the anode outlet pressure decreases to a preset value, e.g. 1.06 bar, the

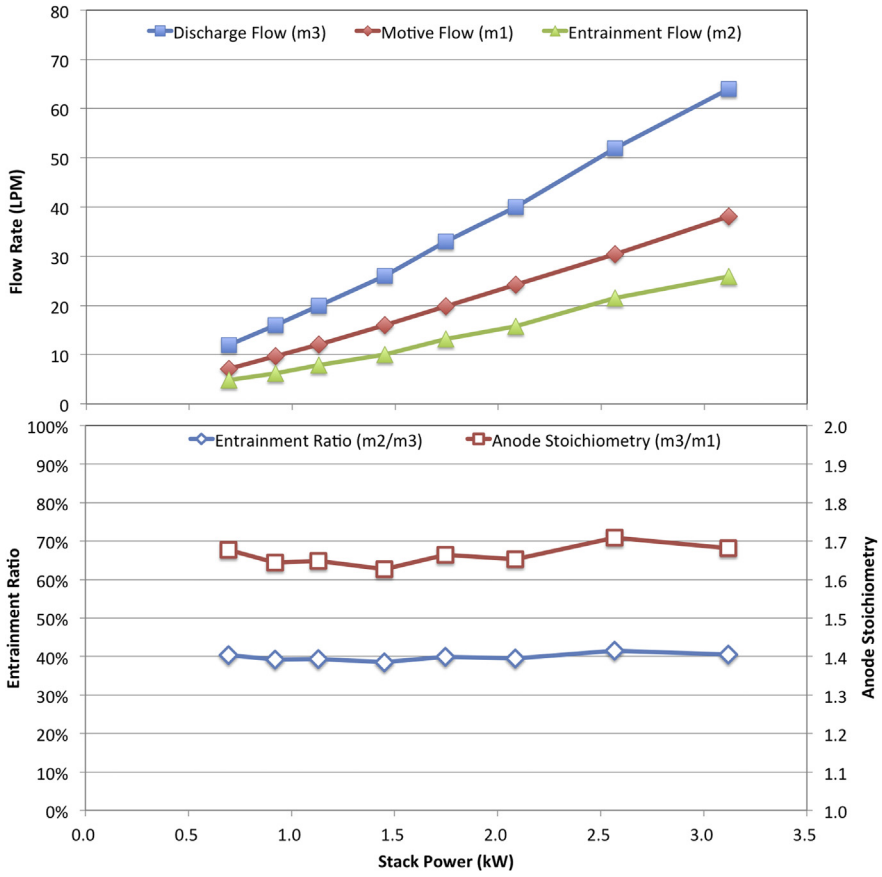

Fig. 6. Hydrogen flow characteristics in the anode for stack power higher than 600 W.

solenoid valve SV1 opens and thus the anode pressure increases again. The periodic opening and closing of the solenoid valve SV1 creates a pulsed hydrogen supply to the ejector and allows more fuel to enter the anode than the actual consumption required by the stack load, which results in a periodic high recirculation rates and some fuel accumulation in the anode loop. This mechanism causes an overall improved fuel recirculation by creating an adequate motive flow in the ejector and a better removal of water droplets from the anode flow field channels. Even if the anode pressure difference drop during the brief periods of time when the solenoid valve SV1 is closed, and as a consequence water accumulates in the fuel cell stack, the increase in the anode pressure difference when the solenoid valve SV1 is next opened will remove the accumulated water from the anode flow field channels.

3.3. *Transient test of the system*

To examine the feasibility of the present passive hydrogen delivery scheme, the transient test of a PEM fuel cell generator using the current technique is carried out. Fig. 8 shows the electrical characteristics of the PEM fuel cell generator under the constant system power of 1.45 kW. It can be seen that the stack power is higher than the system power, typically by about 300 W–600 W. The extra power is mainly used to drive the system auxiliaries and dissipates by the conversion and the transmission losses. The step change in the stack power distribution is mainly caused by the operation of the cathode air blower [18]. The power demand of the air blower is dependent not only on the load operation, but also on the cell voltage. When the cell voltage decreases to an extent, e.g., 0.4 V per cell, the air blower should run in full power mode to blow out the accumulated water inside the cathode. Therefore, the power step is due to the action of the air blower. It can be further seen from Fig. 8 that the stack voltage is confined in a narrow range of 30–36 VDC during the operation period. The dynamics of the current extracted from the stack is relatively significant, ranging from 50 to 65 A. In general, the transient current distribution of the stack current is similar to that of the stack power. It should also be noted that the current extracted from the stack is largely related to the hydrogen flow rates in the stack anode, which will be discussed later.

Fig. 9 shows the transient variations of hydrogen flow rates across the ejector at the system power of 1.45 kW. The motive flow rate *m1* and the discharge flow rate *m3* are directly measured from the mass flow meters, while the entrainment flow rate *m2* is obtained by subtracting the motive flow rate from the discharge flow rate. It is seen that the motive flow rate *m1* is in parallel with the stack current shown in Fig. 8. This is a very reasonable observation considering the electron mass-balance requirements. In addition, the figure also shows that the entrainment flow is relatively stable when the motive flow keeps constant. In contrast, the step-change in the motive flow rate results in a high variation of the entrainment flow rate.

Fig. 10(a) and (b) show the transient variations of the entrainment ratio (*m2*/*m3*) of the vacuum ejector and the hydrogen anode stoichiometry for the PEM fuel cell generator, respectively, under the constant system power of 1.45 kW. It is clearly seen that the entrainment ratio ranges from 30 to 45% during the experiment, which is highly consistent with the measurements shown in Fig. 6. The hydrogen anode stoichiometry ranges from 1.4 to 1.9 with an average of 1.6 during the experiment.

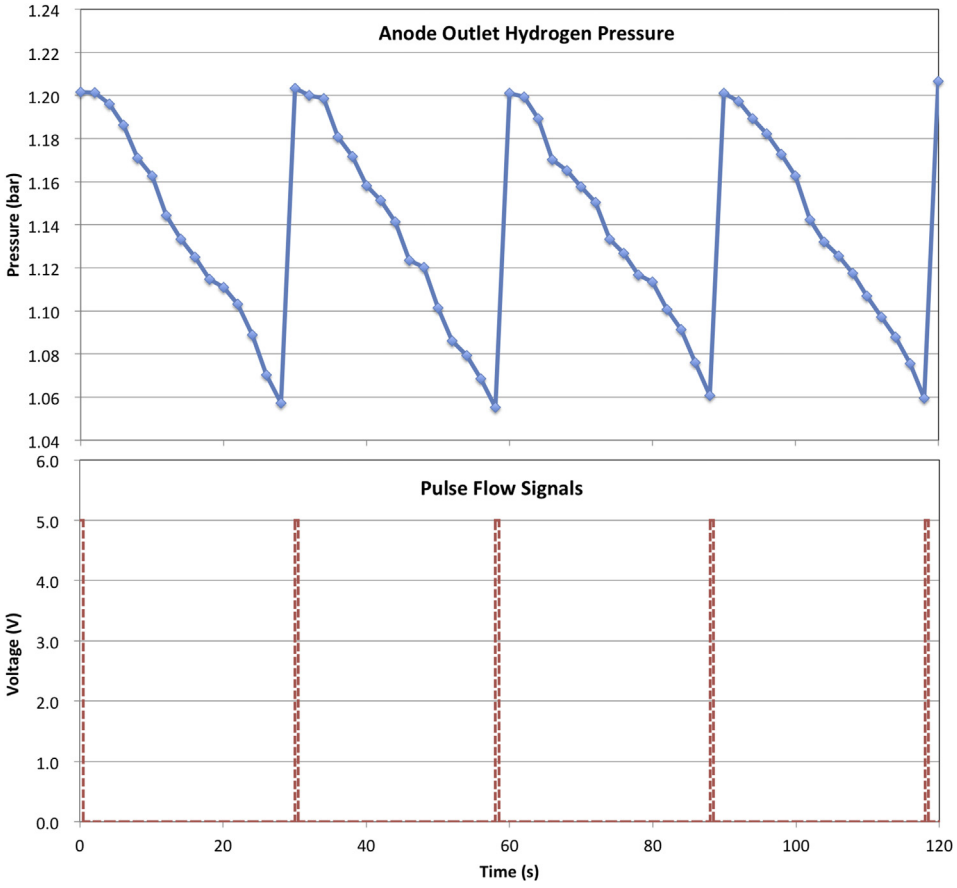

Fig. 7. Anode outlet pressure profiles for purge-flow mode for stack power of 300 W.

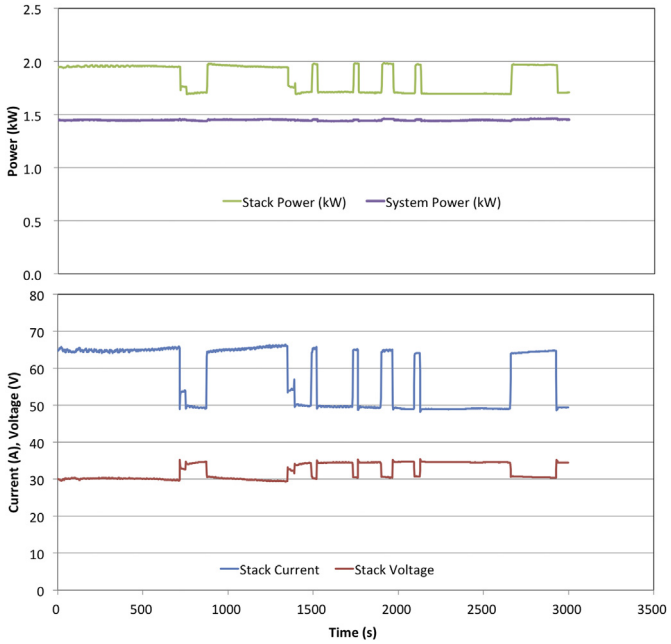

Fig. 8. Transient variations of stack voltage, stack current and stack power at constant system power of 1.45 kW.

3.4. Electrical efficiency

The electrical efficiency of the fuel cell stack is defined as the ratio of the stack gross power (P_{stack}) to the hydrogen power (P_{H2}), i.e.,

$$\varepsilon_{stack} = \frac{P_{stack}}{P_{H2}} = \frac{I_{stack} \times V_{stack}}{C \times m1} \quad (1)$$

where $m1$ is the motive flow of the ejector, and C is a transfer coefficient between the hydrogen flow rate and the power, i.e., 0.1646 kW-LPM^{-1}. The gross power extracted from the fuel cell stack is derived from the measured stack current (I_{stack}) and the stack voltage (V_{stack}). The hydrogen mass flow rate in Eq. (1) is directly measured from the mass flow meter. The electrical efficiency of the fuel cell system can be determined by considering the contributions of stack power, auxiliary power consumption, and power conversion/transmission loss. The present work, however, does not use this approach because it is problematic to measure the transient power consumption of the auxiliaries during the operation. For example, it is not easy to determine the real power dissipation by the air blower, which fluctuates by the speed-up and the slow-down of the motor during the operation. Therefore, the system efficiency is defined as the ratio of the net power to the external load, P_{load}, to the consumed hydrogen power, i.e.,

$$\varepsilon_{system} = \frac{P_{load}}{P_{H2}} = \frac{I_{load} \times V_{load}}{C \times m1} \quad (2)$$

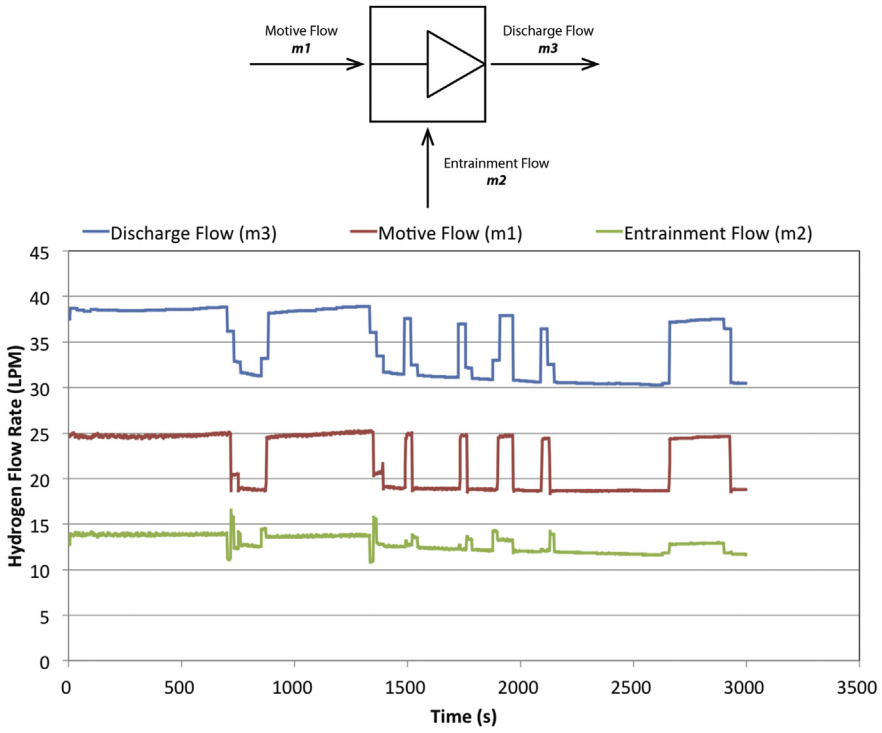

Fig. 9. Hydrogen flow rate for flow across the vacuum ejector at constant system power of 1.45 kW.

where P_{load} is determined by the voltage across the external load (V_{load}) and the current passing through the circuit (I_{load}).

As shown in Fig. 11(a), the transient distribution of the hydrogen power is in parallel with that of the stack power. Moreover, the hydrogen power required for driving the external load 1.45 kW ranges from 3.0 kW to 4.0 kW. The corresponding stack efficiency varies from 47 to 56%. With respect to the system-level result, the electrical efficiency is in the range of 35–47%.

4. Conclusions

In this work, a passive scheme has been deployed to recover the unused hydrogen from the anode outlet of a PEM fuel cell system. A vacuum ejector is employed to fluidly connect the stack anode outlet to entrain the unused hydrogen into the main hydrogen supply. To cover a wide range of stack power consumption, a hybrid scheme combining a continuous supply flow and a pulse supply flow is employed to efficiently recover the unused hydrogen in the anode exhausts. The former flow mode deals with the normal and high stack power conditions, while the latter flow mode is active only when the stack power is beyond the working range of the vacuum ejector. The measurements of the flow and its electrochemical characteristics revealed that the hydrogen anode stoichiometry has been successfully stabilized in the range of 1.4–1.6 under the constant system load of 1.45 kW. The results also showed that the entrainment ratio varies between 40% and 50%. The system efficiency was found to be between 35% and 48%, whereas the stack efficiency varied from 48% to 56% at the system power of 1.45 kW. The transient results reveal that the PEM fuel cell system displays reliable operation without any failure during the approximate 1-h test. This indicates that the stability and the reliability of the present hydrogen recovery scheme are, to a certain extent, satisfactory.

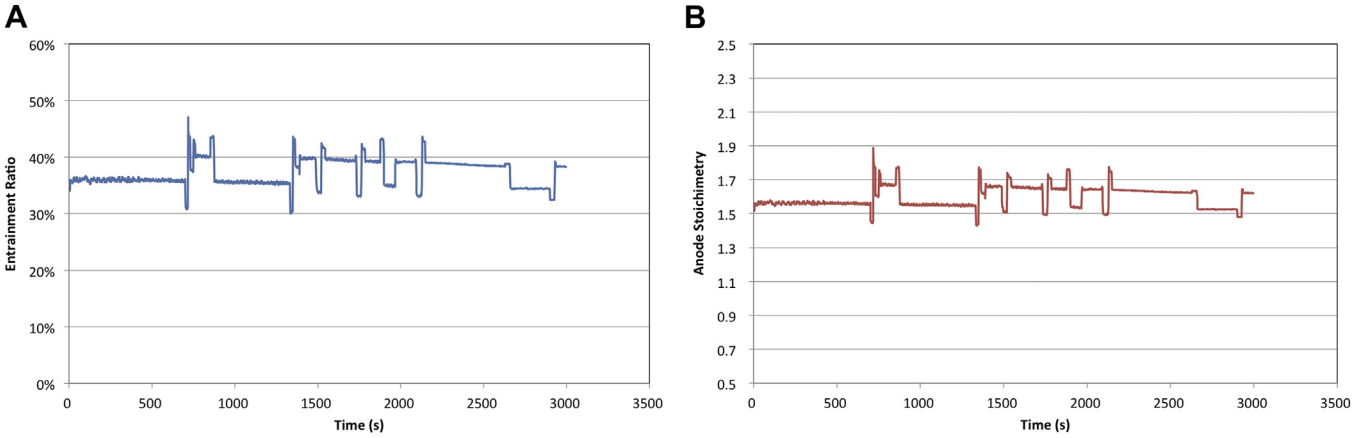

Fig. 10. Transient variations of (a) entrainment ratio ($m2/m3$) and (b) hydrogen anode stoichiometry ($m3/m1$).

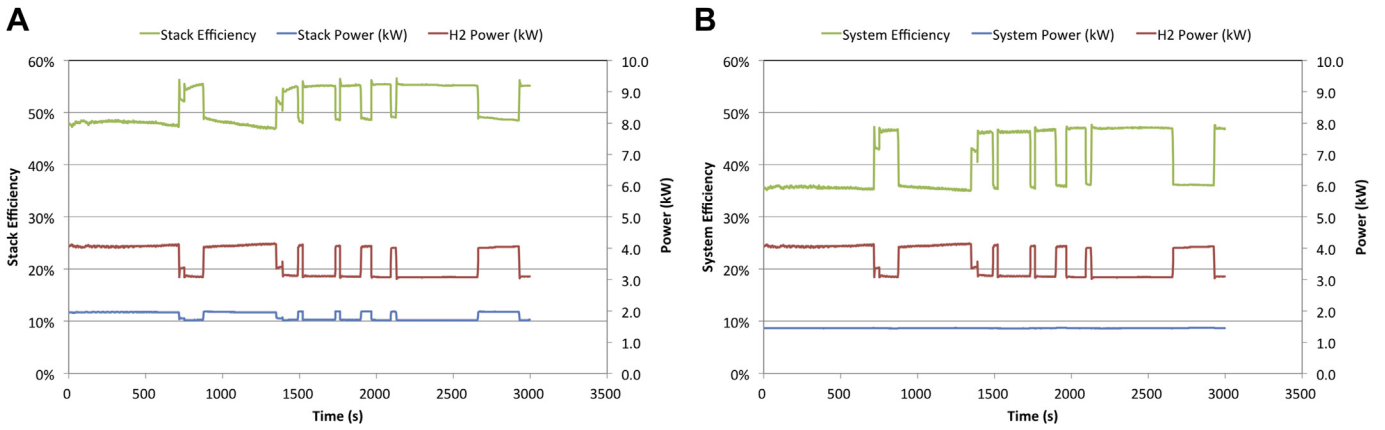

Fig. 11. Transient variations of hydrogen power and the fuel cell efficiencies (a) stack efficiency, and (b) system efficiency.

The entrainment-flow angle relative to the motive flow is an important parameter of the performance of the ejector, which will be discussed in our future efforts.

Acknowledgments

The author professor Jenn-Jiang Hwang would like to thank the National Science Council of Taiwan, for financially supporting this research under contract no. NSC 98-2221-E-024-015-MY2.

References

[1] F. Barbir, PEM Fuel Cells: Theory and Practice, Academic Press, 2012.
[2] R.K. Ahluwalia, X. Wang, J. Power Sources 177 (2008) 167.
[3] S. Hikita, F. Nakatani, K. Yamane, Y. Takagi, JSAE Rev. 23 (2002) 177.
[4] T. Yang, P. Shi, Int. J. Hydrogen Energy 33 (2008) 2795.
[5] J.J. Hwang, D.Y. Wang, N.C. Shih, J. Power Sources 141 (2005) 108.
[6] E.J. Carlson, P. Kopf, J. Sinha, S. Sriramulu, Y. Yang, Cost Analysis of PEM Fuel Cell, TIAX LLC, Cambridge, Massachusetts, 2005.
[7] GM Global Technology Operations LLC, US Patent 8129056 B2, 2012.
[8] T. Sugawara, S. Kizaki, Y. Nuiya, US patent 6858340, 2005.
[9] J.J. McKetta, in: Encyclopedia of Chemical Processing and Design, Taylor & Francis, 1983.
[10] D. Robert, N. Brian, US patent 5441821, 1995.
[11] J.J. Hwang, J. Power Sources 219 (2012) 317.
[12] J.J. Hwang, M.L. Zou, J. Power Sources 195 (2010) 2579.
[13] W.R. Chang, J.J. Hwang, F.B. Weng, A. Su, J. Power Sources 166 (2007) 149.
[14] B. Lin, J. Power Sources 86 (2001) 202.
[15] J.J. Hwang, M.L. Zou, W.R. Chang, A. Su, F.B. Weng, W. Wu, Int. J. Hydrogen Energy 35 (2010) 8644.
[16] D. Chen, W. Li, H. Peng, J. Power Sources 180 (2008) 461.
[17] J.J. Hwang, W.R. Chang, J. Power Sources 207 (2012) 111.
[18] J.J. Hwang, J. Power Sources 223 (2013) 325.
[19] J.J. Hwang, J. Electrochem. Soci 153 (2006) A216.
[20] J.T. Pukrushpan, A.G. Stefanopoulou, H. Peng, Control of Fuel Cell Power Systems: Principles, Modeling, Analysis and Feedback Design, Springer, 2004.
[21] J.J. Hwang, Int. J. Hydrogen Energy 38 (2013) 3727.
[22] J.J. Hwang, J. Power Sources 239 (2013) 54.
[23] D. Frank, X. Chen, US patent 6541141, 2003.
[24] C.J. Geankoplis, Transport Processes and Separation Process Principles, Prentice Hall Professional Technical Reference, 2003.